

Low Complexity Enhanced Hybrid Spectrum Sensing Architectures for Cognitive Radio Equipment

Ziad Khalaf, Amor Nafkha, and Jacques Palicot
SUPELEC/IETR

SUPELEC, Avenue de la Boulaie, CS 47601
35576 Cesson Sévigné Cedex, France

Email: {ziad.khalaf, amor.nafkha, jacques.palicot}@supelec.fr

Mohamed Ghozzi

R-Interface, Ercom Group

9 Grand'Rue 13002 Marseille, France

Email: mohamed.ghozzi@ercom.fr

Abstract—Spectrum sensing enables detecting opportunities in licensed bands in order to access unused portions of the licensed spectrum. In this paper we propose two low complexity detectors based on a combination of two well-known and complementary signal detection mechanisms: energy detection and mono-cycle detection, which exploits cyclostationarity property of the signals. In the first algorithm the mono-cycle detector iteratively corrects the thresholds of a double threshold energy detector, that will finally converge to the performance of the mono-cycle detector. The second algorithm uses the mono-cycle detector to directly estimate the noise level N_0 , which is used to fix the threshold of the radiometer. Simulation results conducted on different environments show promising performances of the proposed detectors especially in low SNR .

Index Terms—Cognitive Radio, Spectrum sensing, Energy detector, Detection features.

I. INTRODUCTION

The term ‘‘Cognitive Radio’’, defined by J.Mitola [2] was reused by the FCC [3] to define a class of radio systems that continuously perform spectrum sensing, dynamically identify vacant (unused) spectrum and then operate in this spectrum at a time when it is not used by incumbent radio systems.

The increasing in telecommunication services number and rates has led to a growing demand of spectrum resources. The objective of cognitive terminals is to obtain independently and dynamically radio frequencies to access the network. Large parts of the spectrum allocated to licensed radio services (referred to as primary users, PUs) have exclusive access rights. However, secondary users (SUs) can still access opportunistically to the spectrum held by the PUs when they are not using it.

As they do not have full access rights, SUs must guarantee to not cause harmful interference to PUs. Hence they need to monitor the spectrum continuously to detect if PUs resumed their communications. For that purpose, it has been suggested by the FCC to use Cognitive Radio based technology to help SUs filling these requirements. In that case Cognitive Radios (CRs) must stop and transfer their activities to another vacant band. CRs need to be more sensitive than PUs and efficient at lower SNR to detect PUs signals.

Various spectrum sensing techniques have been presented as noticed in [4] including *the classical likelihood ratio test (LRT)* [5], *energy detection (ED)* [5]–[7], *matched filtering (MF) detection* [5], [8], *cyclostationary detection (CSD)* [9]–[13], and some newly emerging methods such as *eigenvalue-based sensing* [14]–[16], *wavelet-based sensing* [17], *covariance-based sensing* [18], and *blindly combined energy detection* [19]. In this paper, our focus is on energy and cyclostationary detection. However, for other different methods of spectrum sensing in cognitive radio, we advise the readers to refer to [4], [20]. Energy detection is the simplest detection method but needs the exact knowledge of the noise level N_0 ; furthermore, a wrong estimation is known to seriously impact the detection performance [6]. Cyclostationary detection was proposed as an alternative since noise is stationary whilst telecommunication signals are rather cyclostationary. The advantage of cyclostationary methods is that it does not need any knowledge about the noise level N_0 and allows the detection at low SNR . However, one major drawback of cyclostationary detection is that it requires high computation time and needs a high sampling rate. In this paper, we propose a modified version (M-HSD) of the HSD proposed in [1], and an Enhanced HSD (EHSD) algorithms that combine cyclostationary and energy detection, to detect the free spectrum. Taking into consideration the limitations of the energy detector performance due to presence of noise uncertainty and background interference, the idea of this paper is to reduce the uncertainty over the noise level N_0 using the help of cyclostationary detection. Two kind of strategies can be applied, the first one (M-HSD) uses an iterative approach: at the beginning of the sensing, we can usually fix two thresholds ξ_1 and ξ_2 for the energy detector. Then, the detection is given by the following process: if the energy detector criteria is greater (*resp.* smaller) than ξ_2 (*resp.* ξ_1) then this indicates the presence (*resp.* absence) of the primary user signal. Else if the energy detector criteria is inside the interval $[\xi_1, \xi_2]$, then cyclostationary detection can be applied and based on its decision, the hybrid architecture can iteratively adjust the thresholds of the energy detector, to finally converge to the performance of the cyclostationary

detector. The second approach (EHSD) consists in directly estimating the noise level N_0 using the cyclostationary detector and uses this estimation to obtain the appropriate threshold of the radiometer.

The remaining part of the paper is organized as follows. In Section II, we present the system model adopted throughout this work. We briefly describe energy and cyclostationary detectors in Section III. The proposed HSD architecture will be recalled in Section IV. The M-HSD architecture will be presented in Section V. In section VI, EHSD algorithm is proposed. Section VII presents simulation results and discussions. Finally, Section VIII presents the conclusions of this study and makes some suggestions for future work.

II. SYSTEM MODEL

The spectrum sensing detection problem consists of collecting a set of N samples y_1, y_2, \dots, y_N from a given frequency band B , processing the data by a Neyman-Pearson receiver, which takes the form of a Likelihood Ratio Test (LRT) and deciding for that frequency band whether or not a primary user is present. Let \mathbf{y} denotes the vector formed by N samples, $\mathbf{y} = [y(1), \dots, y(N)]^t$, where the samples are realizations of the random variables Y_1, Y_2, \dots, Y_N , respectively. The LRT compares a statistic λ to a fixed threshold ν . The statistic λ is the ratio between the joint Probability Density Function (PDF), $p_Y(\mathbf{y}|H_1)$, of the N samples given that a primary user is present and the joint PDF, $p_Y(\mathbf{y}|H_0)$, of N samples given that no primary user is present. H_1 and H_0 denote the binary hypotheses that a primary user is present and absent, respectively. This ratio is called Likelihood Ratio (LR). The threshold ν is determined by constraining the probability of false alarm to a specified value.

The binary hypotheses (H_0, H_1) are defined in a way such that, under hypothesis H_1 and $k \in [1, \dots, N]$, the k^{th} collected sample, $y(k)$, is composed of a primary user signal sample, $x(k) \sim \mathcal{N}(0, \sigma_x^2)$, affected in different ways by the channel, $h(k) \sim \mathcal{N}(0, 1)$, plus an additive Gaussian noise sample, $n(k) \sim \mathcal{N}(0, \sigma_n^2)$, where $\mathcal{N}(m, \sigma^2)$ denotes the normal distribution with mean m and variance σ^2 . Under hypothesis H_0 , the k^{th} sample, $y(k)$, consists of the additive Gaussian noise sample $n(k)$. Hence,

$$\begin{cases} H_0 : y(k) = n(k) \\ H_1 : y(k) = h(k)x(k) + n(k) \end{cases}$$

The LRT then takes the form

$$\lambda = \frac{p_Y(\mathbf{y}|H_1)}{p_Y(\mathbf{y}|H_0)} \underset{H_1}{\lesssim} \nu \underset{H_0}{\gtrsim}$$

For $\lambda > \nu$, H_1 is decided, otherwise H_0 is decided. Assuming that the samples are statistically independent, the joint PDF $p_Y(\mathbf{y}|H_i)$; $i \in \{0, 1\}$, is nothing but the product of the N marginal PDFs of the samples. Specifically,

$$p_Y(\mathbf{y}|H_i) = \prod_{k=1}^N p_{Y_k}(y_k|H_i); i \in \{0, 1\}$$

The performance of any spectrum sensing methods is indicated by two probabilities: the detection probability, P_d , which defines the probability of the sensing algorithm having detected the presence of the primary signal under the hypothesis H_1 ; probability of false alarm, P_{fa} , which defines the probability of the sensing algorithm claiming the presence of the primary signal under the hypothesis H_0 . In the hypothesis testing problem, where we have to decide whether the primary signal is present or absent, two kinds of errors can occur:

- A false alarm occurs when it is decided that the primary signal is present even though it is not.
- A miss detection occurs when it is decided that the primary signal is not present even though it is.

The performance, of sensing algorithm, is usually presented using a family of curves showing the detection probability P_d as function of the false alarm probability P_{fa} (Cf. Figure 1). The test is good when these curves are located above the chance line that characterizes pure hazard. In literature, this representation is called ROC curve (Receiver Operational Characteristic) [21].

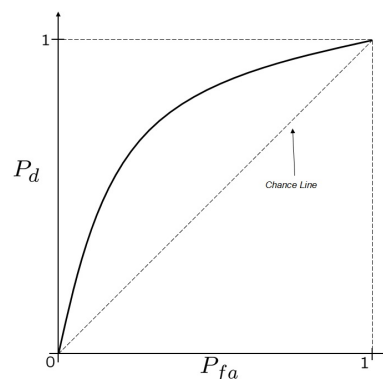


Fig. 1. Example of ROC curve showing the probability of detection P_d according to the probability of false alarm P_{fa}

III. SENSING METHODS

A. Generalities

The optimal sensing detector needs to know the values of channels gain, noise and primary user's variance. In practice, we may have no knowledge about the values of some or all of these parameters. In these cases, an approximation of the optimal test is done in the case of Gaussian signals with low level compared to noise (assumed white and Gaussian). It is given by the locally optimal test [21], which uses only second order statistics of the signal. Application of Taylor's theorem yields the following statistical test:

$$Z = \frac{1}{N_0^2 T} \int_{-T/2}^{T/2} \int_{-T/2}^{T/2} R_{xx}(u, v) y(u) y(v) du dv \underset{H_1}{\lesssim} \xi \underset{H_0}{\gtrsim} \quad (1)$$

With $R_{xx}(u, v)$ is the autocorrelation function and T is the listening duration before the detector takes any decision. Thus, the new detector calculates a quadratic transformation of

the received signal and compares the result to a detection threshold. However, in the case of low SNR, it is shown in [22] that this locally optimal detector remains valid even in the case where the signals of interest are not Gaussian. Depending on the chosen statistical model of the observation $x(t)$, two types of detectors can be derived. For a stationary model, the detector is the energy detector or radiometer. It is a simple detector with low complexity and reduced time of computation, but has the disadvantage of being sensitive to a bad estimate of the noise level N_0 . For a cyclostationary model of $x(t)$, the detector is the mono or multi-cycles detector. This detector is able to detect in low SNR, and is insensitive to the poor estimate of noise level, but has the disadvantage of an important computing time.

B. Energy Detection

When the statistical model of the signal of interest $x(t)$ is chosen to be stationary, the autocorrelation function $R_{xx}(u, v)$ becomes dependent only of the difference $u - v$ and it can be written under this form: $R_{xx}(u, v) = R_{xx}(u - v)$.

By performing variable changes according to:

$$\begin{aligned} u &= t + \frac{\tau}{2} \\ v &= t - \frac{\tau}{2} \end{aligned} \tag{2}$$

we obtain the following local optimal detector form [23]:

$$Z_{ro} = \frac{1}{N_0^2} \int_{-\infty}^{\infty} R_{xx}(\tau) R_{yy}(\tau)_T d\tau \tag{3}$$

where $R_{yy}(\tau)_T$ is the correlogram of $y(t)$ defined by :

$$R_{yy}(\tau)_T \triangleq \begin{cases} \frac{1}{T} \int_{-(T-|\tau|)/2}^{(T-|\tau|)/2} y(t - \frac{\tau}{2}) y(t + \frac{\tau}{2}) dt, & |\tau| \leq T \\ 0 & \text{elsewhere} \end{cases}$$

Using the Parseval theorem [5] applied to (3), the statistical test becomes:

$$Z = \frac{1}{N_0^2} \int_{-\infty}^{\infty} S_{xx}(f) P_T(f) df \tag{4}$$

With $P_T(f)$ the peridogram of $y(t)$ given by:

$$P_T(f) = \frac{1}{T} | Y_T(f) |^2$$

and

$$Y_T(f) = \int_{-T/2}^{T/2} y(t) \exp^{-i2\pi ft} dt$$

Hence the local optimal detector computes the periodogram of the observed signal $y(t)$. The obtained result is then correlated with the ideal. Since the power spectral density $S_{xx}(f)$ cannot be known *a priori*, we replace it in (4) by a non zero constant S_0 over all the band $[-B/2, B/2]$ of the received signal to obtain the new statistical test:

$$Z_r = \frac{S_0}{N_0^2} \int_{-B/2}^{B/2} P_T(f) df \tag{5}$$

The obtained detector is called radiometer or energy detector whose statistical test is proportional to the energy of the

received signal. The application of the Parseval theorem to (5) results in the following statistical test in the time domain:

$$Z_r \propto \frac{1}{T} \int_0^T y(t)^2 dt \tag{6}$$

Where the symbol \propto indicates proportionality. Urkowitz [7] studied the energy detector with the statistic test X , which is equal to second term of equation (6). The block diagram of a radiometer is given in Figure 2. Urkowitz studied also the expression of the probability density function of the statistic X and showed that for a large time-bandwidth product ($BT > 250$) the statistic X follows a Gaussian law under both conditions: noise alone, or signal plus noise, with mean μ_{j+1} and variance σ_{j+1}^2 ($j \in \{0,1\}$) given by:

$$\begin{aligned} H_0 \quad \mu_1 &= N_0 BT, & \sigma_1^2 &= N_0^2 BT \\ H_1 \quad \mu_2 &= N_0 BT(SNR + 1), & \sigma_2^2 &= N_0^2 BT(2SNR + 1) \end{aligned} \tag{7}$$

where SNR refers to the *signal to noise ratio* defined as:

$$SNR = \frac{E_x}{N_0 B}$$

with E_x the power of the signal $x(t)$ over the duration T . The probability of detection P_d and of false alarm P_{fa} becomes:

$$P_{fa} = Q \left\{ \frac{\xi - \mu_1}{\sigma_1} \right\}$$

and

$$P_d = Q \left\{ \frac{\xi - \mu_2}{\sigma_2} \right\}$$

with

$$Q(u) = \frac{1}{\sqrt{2\pi}} \int_u^{\infty} \exp^{-v^2/2} dv$$

Then, for a desired false alarm probability $P_{fa,des}$, we can compute the adequate detection threshold ξ_0 using the following equation:

$$\xi_0 = \mu_1 + \sigma_1 Q^{-1}(P_{fa,des}) = G(P_{fa,des}) N_0 \tag{8}$$

with:

$$G(P_{fa,des}) = BT + \sqrt{BT} Q^{-1}(P_{fa,des})$$

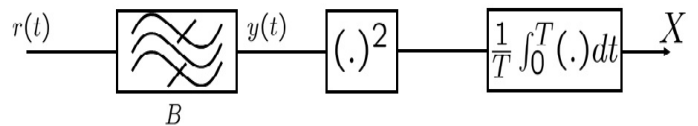


Fig. 2. Block scheme of the energy detector.

1) *Energy detection limits:* The good performance of the radiometer is accurate if the noise spectral density N_0 is perfectly known at the receiver. In a classical communication between transmitter and receiver, there is a preliminary exchange of data, which are known by the receiver, who is able to determine a good estimation of the noise level N_0 . This cooperative aspect between transmitter and receiver is unfortunately absent in the case of detection of free bands because no data exchange is driven between terminals in opportunistic radio access. Subsequently, the estimated noise level \hat{N}_0 is not exempt from error especially when the tested band is occupied. As the detection threshold is proportional to N_0 (Cf. (8)), it can not be determined with accuracy, leading to more degradation of the radiometer performance.

2) *Ideal Radiometer Performance:* Let $P_{d,des}$ designate, the desired detection probability, $u' = Q^{-1}(P_{d,des})$ and $v' = Q^{-1}(P_{fa,des})$. It is shown in [6] that for large time-bandwidth product BT , the minimum signal to noise ratio snr_m that guarantees a desired probability of false alarm $P_{fa,des}$ and a desired probability of detection $P_{d,des}$ is given by:

$$snr_m = \frac{v'}{\sqrt{BT}} + \frac{u'}{BT} \left[u' - \sqrt{u'^2 + BT + 2v'\sqrt{BT}} \right]$$

The variation of this ratio depends on the time-bandwidth product BT as shown in Figure 3.

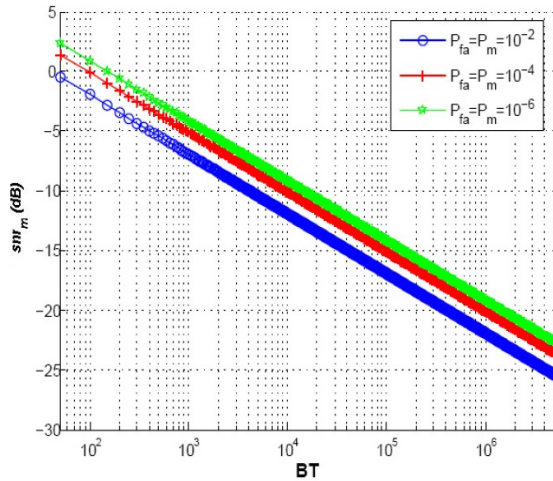


Fig. 3. the variation of the minimum signal to noise ratio snr_m that guarantees the desired probability of false alarm P_{fa} and a desired probability of miss detection P_m , versus the time-bandwidth product BT . When the noise level N_0 is perfectly known, snr_m decreases as the product BT increases.

For different values of probability $P_{fa,des}$ and probability of detection $P_{d,des}$, the required snr_m for detection decreases as the time-bandwidth product BT increases. It should be noted that BT is proportional to the number of observations available when the received signal is sampled.

3) *Non Ideal Radiometer:* Let \hat{N}_0 be an estimated value of the noise level N_0 and $\hat{\xi}_0$ the corresponding threshold of detection. In the case of an under-estimation of N_0 i.e., $\hat{N}_0 < N_0$, Figure 4 shows that a bad decision is performed when

the energy X of the signal is located in the interval $[\hat{\xi}_0, \xi_0]$. In the case of free bands detection, this bad decision results in the declaration of an occupied strip while it is free, causing an increase of the probability of false alarm.

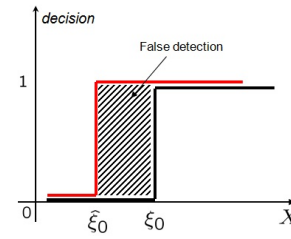


Fig. 4. Decision error in the case of an under-estimation of noise level N_0 . This bad decision results in the declaration of an occupied strip while it is free, causing an increase of the probability of false alarm.

However, in the case of an over-estimation of noise level N_0 i.e., $\hat{N}_0 > N_0$, Figure 5 shows that a wrong decision is made when the energy of the received signal X is located in the interval $[\xi_0, \hat{\xi}_0]$. In terms of free bands detection, this error results in declaring that the tested band is free, while it is occupied, which provides a more important missing probability. Consequently, the uncertainty on the noise level

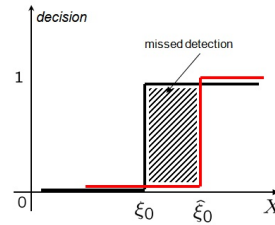


Fig. 5. Decision error in the case of an over-estimation of noise level N_0 . This error results in declaring that the tested band is free, while it is occupied, which provides a more important missing probability, and causes interference to the PU.

leads in one case to an under-exploitation of free bands by secondary users and in another case to more interferences generated to the primary users. To overcome undesirable effects of uncertainty on the value of N_0 , it has been proposed in [6] to use a different detection threshold given by:

$$\hat{\xi}_0 = U\xi_0$$

Where U is the peak-to-peak uncertainty on the estimation of noise level N_0 given by:

$$U = \frac{1 + \epsilon_2}{1 - \epsilon_1} \geq 1$$

Here, ϵ_1 and ϵ_2 give the range of uncertainty on the estimation of N_0 :

$$(1 - \epsilon_1)N_0 \leq \hat{N}_0 \leq (1 + \epsilon_2)N_0$$

Thus, the expression of snr_m [6] becomes:

$$snr_m \approx (U - 1) + O\left(\frac{1}{\sqrt{BT}}\right)$$

The term $(U - 1)$ determinates the minimum SNR under, which detection is more regardless of possible parameters $P_{fa,des}$, $P_{d,des}$ and the observation time T of the detector. In the particular case where $P_{fa,des} = 1 - P_{d,des} = 0.01$, Figure 6 shows the evolution of the snr_m as a function of BT for different values of U . Whatever U nil or not, the value of snr_m decreases as the BT product increases. In contrast, if $U \neq 0$ (presence of uncertainty), the decay tends asymptotically to its limit $U - 1$. For example, for $U = 3$ dB, the value of snr_m limit is 2 dB. Despite its low complexity and ease of implementation, the radiometer does not perform a reliable detection of free bands especially if the uncertainty regarding the noise level is important or the SNR is low.

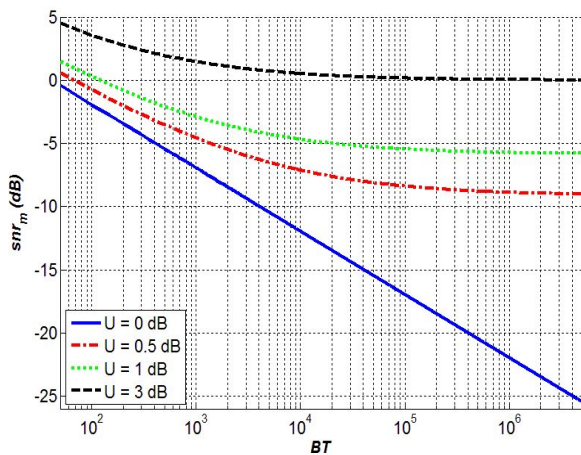


Fig. 6. When the value of U is different from zero (presence of uncertainty), the value of snr_m decreases as the BT product increases, and tends asymptotically to its limit $U - 1$.

C. Cyclostationary Detection

When the cyclostationary model is adopted for the signal of interest $x(t)$, the autocorrelation function $R_{xx}(u, v)$ is expressed as a function of the cyclic autocorrelation

$$R_{xx} = \sum_{\alpha} R_{xx}(\alpha, u - v) \exp^{i\pi\alpha(u+v)} \quad (9)$$

By replacing $R_{xx}(u, v)$ in (1) by its expression in (9), and by performing variables changes according to (2), we obtain the statistical test of the multi-cycle's coherent detector:

$$Z_{mc} = \sum_{\alpha} \frac{1}{N_0^2} \int_{-B}^B R_{xx}(\alpha, \tau)^* R_{yy}(\alpha, \tau)_B d\tau$$

With $R_{yy}(\alpha, \tau)_B$ is the cyclic periodogram of the observation $y(t)$ whose expression is presented in [24]. The local optimal detector computes the correlogram of the observation over all cyclic frequencies contained in the detected signal and the obtained result is then correlated with the ideal cyclic autocorrelation of the expected signal.

In the frequency domain after applying Parseval's theorem, this statistic test is written as follows:

$$Z_{mc} = \sum_{\alpha} \frac{1}{N_0^2} \int_{-\infty}^{\infty} S_{xx}(\alpha, f)^* S_{yy}(\alpha, f)_B df$$

With $S_{yy}(\alpha, f)_B$ is the cyclic periodogram of the observation $y(t)$. In practice, the implementation of the multi-cycles detector is impossible due to the non-knowledge of the ideal functions $R_{xx}(\alpha, \tau)$ or $S_{xx}(\alpha, \tau)$ of the signals to detect. In fact, their phases can not be known in advance because the expected signals are random. To overcome this indeterminacy on the phase, two alternatives are possible [24]. In the first alternative, the implementation of the statistic Z_{mc} occurs in an adaptive manner. This means that for each calculation of Z_{mc} , a phase search is made according to the maximization of the statistic Z_{mc} . If this is not enough, a second alternative is to detect a single frequency at a time:

$$Z_{\alpha} = \left| \int_{-\infty}^{\infty} S_{xx}(\alpha, f)^* S_{yy}(\alpha, f)_B df \right| \underset{H_1}{\overset{H_0}{\gtrless}} \xi$$

For $\alpha = 0$, the obtained detector is the optimal radiometer. For $\alpha \neq 0$, the detector is called coherent mono-cycle detector. In a noisy environment of a known spectral density N_0 , Gardner [10] and Izzo [25] show that, the optimal radiometer detector (with perfect knowledge of N_0) is better than the coherent mono-cycle detector. In [26], different noise models was considered: Gaussian, non-Gaussian, white and non-white. The author concluded that in a realistic situation characterized by a variable noise level, the optimal performance of the radiometer is becoming significantly degraded and significantly lower than those of mono-cycle detector. Furthermore, the author shows the superiority of mono-cycle detector in a noisy environment characterized by additive interference. In literature, many other cyclic methods of detection / estimation exist. For example, Zivanovic and Gardner [11] define the degree of cyclostationarity of a random process by:

$$DCS = \frac{\sum_{\alpha \neq 0} \int_{-\infty}^{\infty} |R_{xx}(\alpha, \tau)|^2 d\tau}{\int_{-\infty}^{\infty} |R_{xx}(0, \tau)|^2 d\tau}$$

It involves measuring the distance between the correlation of the process of interest and the correlation of the most close stationary process. We can also define the degree of cyclostationarity to a process on a specific frequency α by:

$$DCS^{\alpha} = \frac{\int_{-\infty}^{\infty} |R_{xx}(\alpha, \tau)|^2 d\tau}{\int_{-\infty}^{\infty} |R_{xx}(0, \tau)|^2 d\tau}$$

Although the authors of [11] did not mention the problem of detection, this notion of degree of cyclostationarity can be useful for detection by comparing DCS (or DCS^{α}) to a threshold value given by a criterion such as P_{fa} is constant. Hurd and Gerr [27] proposed a test for the presence of cyclostationarity based on the calculation of the normalized spectral correlation:

$$\gamma(\alpha_p, \alpha_q, M) = \frac{|\sum_{m=0}^{M-1} I_N(\alpha_{p+m}) I_N^*(\alpha_{q+m})|^2}{\sum_{m=0}^{M-1} |I_N(\alpha_{p+m})|^2 \sum_{m=0}^{M-1} |I_N(\alpha_{q+m})|^2}$$

with $I_N(\alpha) = \sum_{n=0}^{N-1} x(n)exp(-i\pi\alpha)$, $\alpha_k = 2\pi k/N$ and M a smoothing parameter. The presence on the plot of $\gamma(\alpha_p, \alpha_q, M)$ varying with α_p of dark lines parallel to the diagonal indicate the cyclostationarity of the signal $x(t)$. Hence the detection is performed in a visual manner.

Dandawate and Giannakis [13] proposed tests for the presence of cyclostationarity at a given frequency based on the following decision rule:

$$Z \propto \hat{C}_{kx}^{(T)} \Sigma_{kx}^{-1} \hat{C}_{kx}^{(T)'} \underset{H_1}{\overset{H_0}{\gtrless}} \xi_G$$

where $\hat{C}_{kx}^{(T)}$ is an estimation vector of the k^{th} order cumulants of the process $x(t)$, $\hat{C}_{kx}^{(T)'}$ the transpose of the vector $\hat{C}_{kx}^{(T)}$, Σ_{kx} the covariance matrix of $\hat{C}_{kx}^{(T)}$ and ξ_G the detection threshold. Unlike the two previous methods, the authors find the distribution of the statistic Z under the two hypotheses H_0 and H_1 . This allows, thereafter, to calculate for a given probability of false alarm the appropriate threshold ξ_G . Very present in the literature, this test is used in the recognition of standards accessible to software radio terminals [28] or in the detection of free channels on the GSM frequency band [29]. In these examples, systems to be detected are *a priori* known permitting a cyclostationarity test over a reduced number of frequencies. In this paper, we choose to retain this test of cyclostationarity to be the cyclic detector used in our different proposed solutions, which will be discussed in the next sections.

D. Limits of the sensing methods

The last two methods (Energy and cyclostationary detection) present many advantages but have some limits; in fact when a band is tested, the detection system delivers a decision such as free or occupied band, without giving more details on the contents of this band in particular in the case of occupation of this band. However, a band may not be completely occupied *i.e.*, sub-intervals of this band are free as we can see from the example of Figure 7. Subsequently, a limitation of this solution is that existing communication opportunities may be missed when the tested bandwidth is much larger than the size of these opportunities.

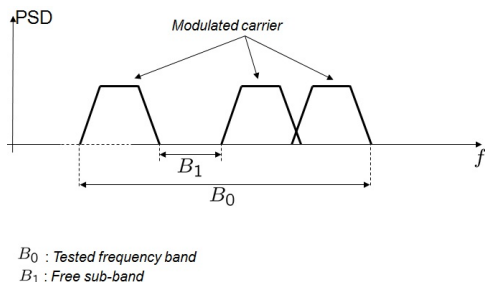


Fig. 7. Example of missed opportunity for communication in the case of a large tested range of frequencies

IV. HYBRID DETECTOR

A. Generalities

As we have seen in Section I, the secondary user undertakes to not create interference to primary users by unwanted access to their frequency bands. For that purpose, secondary users have to perform periodic verifications of these bands. The more often these verifications are done, the lower becomes the risk of interference. Subsequently, periodic scanning of the spectrum is subjected to time constraint especially that the number of bands shared with the primary user can be important.

	Computational complexity	insensitivity of noise	<i>a priori</i> knowledge	Detection in low SNR
radiometer	+	-	noise level N_0	-
cyclostationary Detector.	-	+	cyclic frequencies	+

TABLE I
COMPARISON OF PROPERTIES OF ENERGY (RADIOMETER) AND CYCLOSTATIONARY DETECTOR. THE (+) INDICATES A ADVANTAGE AND (-) INDICATES AN INCONVENIENT

B. detector architecture

Table I gives features comparison between energy and cyclostationarity detectors. Except its noise sensitivity, which degrades its detection in low SNR, energy detector is the best solution to detect free bands because no *a priori* information is needed. Furthermore, it is a very simple method to implement. On the contrary, cyclostationarity detection is very robust but computationnaly extensive and needs the prior knowledge of cyclic frequencies in order to take a quick decision. If this information is unknown, the process becomes too much complicated and it will not be possible to implement it (today) in a real time manner. However, reading carefully table I, it appears that these two methods are complementary. Therefore it is the reason why we propose our hybrid architecture in [1], which permits to detect quickly with minimum *a priori* information free bands, by taking advantage of both methods. This hybrid architecture, which is presented in Figure 8 is an iteratively adaptative architecture as it is explained in [1]. In the next section we introduce the M-HSD algorithm, which is the same as the HSD proposed in [1] but this time we added *buffer*₁ and *buffer*₂ in order to take soft decisions over the modifications of the thresholds ξ_1 and ξ_2 . The benefit of using buffers gives stability for operating at low SNRs as it is explained in the next section.

V. DECISION RULE OF THE M-HSD ALGORITHM

We first assume that N_0 is constant with respect to time. Let X_i be the energy of the received signal $x(t)$ during an observation time T after the iteration i , B the bandwidth of the tested band, ξ_1 and ξ_2 two thresholds that are first initialized at 0 and $+\infty$ respectively. ξ_G , which is the threshold of the

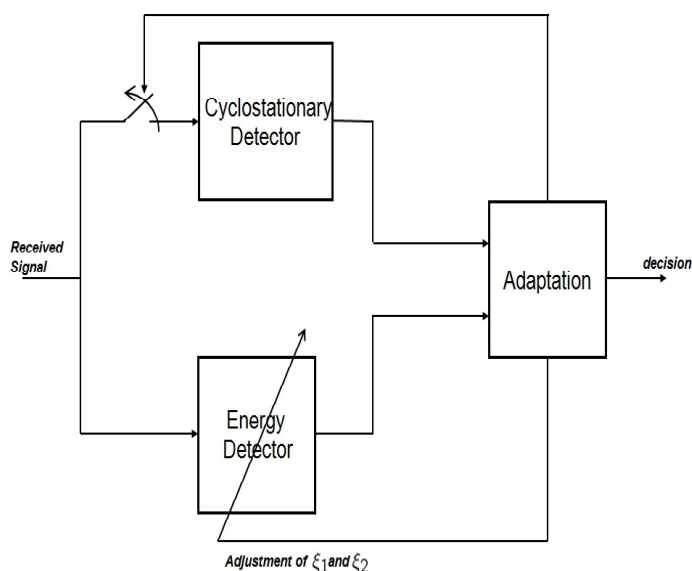


Fig. 8. Hybrid Spectrum sensing Detector (HSD) architecture as it was proposed in [1].

cyclostationary block that is defined in order to respect the desired $P_{fa,des}$, is fixed using the central χ^2 table as described in [13].

At the beginning of the sensing, the energy detector calculates the energy X of the received signal after an observation time T . Then if X falls inside the interval $[\xi_1, \xi_2]$, the energy detector can not make a direct decision of type *signal present* or *signal absent*. In that case, the adaptation stage presented in Figure 8 will call the cyclostationary block (which *a priori* knows the cyclic frequency α of the signal of interest) to make the decision. After the decision of the cyclic test is taken, if it is of the type *signal present* (resp. *signal absent*), the calculated value X is then saved in a buffer called $buffer_2$ of size N_2 , (resp. $buffer_1$ of size N_1).

The algorithm continues in the same way except when $buffer_2$ (resp. $buffer_1$) is full. In this case, the adaptation stage starts to modify the value of the threshold ξ_2 (resp. ξ_1) according to the average of $buffer_2$, (resp. $buffer_1$) and then the oldest value in the buffer will be replaced by the new calculated one (X_i after the iteration i).

At any time, if the calculated value X is outside the interval $[\xi_1, \xi_2]$, the adaptation stage will take automatic decision of type *signal absent* (resp. *signal present*) depending on whether X is less than ξ_1 (resp. greater than ξ_2) avoiding the use of the cyclic test.

The process is repeated making the interval $[\xi_1, \xi_2]$ smaller and smaller. Two cases, high and low SNR , need to be studied in order to analyze the M-HSD architecture limits, which will be explained in the next paragraph. Figure 9 shows the algorithm of the M-HSD method.

It should be noted that at low SNR , the test of “Dandawate and Giannakis” can easily make errors (the two types of errors described in part II), so the values that should be saved in $buffer_1$ might be saved in $buffer_2$ and inversely. But the

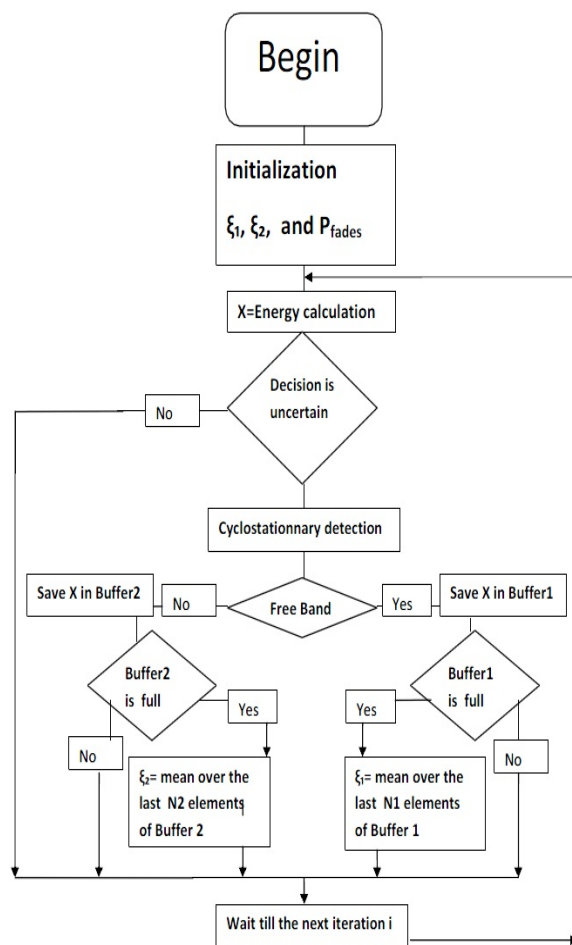


Fig. 9. The M-HSD algorithm (a Modified version of the HSD algorithm [1]). The major modification is the addition of $buffer_1$ and $buffer_2$ in order to make soft modifications over ξ_1 and ξ_2 .

use of buffers can make a “dilution” of these errors over the values of ξ_1 and ξ_2 .

Using the M-HSD algorithm, will practically reduce the complexity from that of a cyclostationary detector: $O(N^2 + 0,5N \log_2 N)$, before the buffers are full, to the one of a radiometer: $O(N \log_2 N)$ at the convergence phase. At this point, the M-HSD detector will present a detection performance close to that of the cyclostationary detector.

A. Analytical Study of the M-HSD algorithm Using Order Statistics

In this section, for simplicity reasons, we assume that the buffers’ size is one. In order to study the M-HSD architecture in a statistical point of view, we will use the order statistics tool. The K^{th} order statistic of a statistical sample denoted $X_{(k)}$ is equal to its K^{th} smallest value. The first order statistic (or smallest order statistic) is always the minimum of the

sample, that is:

$$X_{(1)} = \min\{X_1, \dots, X_n\}$$

Similarly, for a sample of size n , the n^{th} order statistic (or largest order statistic) is the maximum, that is:

$$X_{(n)} = \max\{X_1, \dots, X_n\}$$

if $f(x)$ is the probability density function of the random variable X and $F(x)$ its cumulative distribution function, then it is shown in [30] that the density probability of the k^{th} order statistic is given by:

$$f_{X_{(k)}}(x) = \frac{n!}{(k-1)!(n-k)!} F(x)^{k-1} (1-F(x))^{n-k} f(x) \quad (10)$$

for the special case $k = 1$, (10) becomes:

$$f_{X_{(1)}}(x) = n[1 - F(x)]^{n-1} f(x) \quad (11)$$

and for $k = n$, (10) becomes:

$$f_{X_{(n)}}(x) = nF(x)^{n-1} f(x) \quad (12)$$

Now, using the distributions of X under H_0 (resp. X under H_1) from (7) in (11) (resp. (12)), we can obtain the distributions of ξ_1 and ξ_2 (in (13) and (14) respectively) after n iterations of the algorithm M-HSD under the hypotheses H_0 and H_1 respectively:

$$f_{\xi_1(k=1)}(x) = \frac{n}{2\sigma_1\sqrt{2\pi}} \left[1 + \operatorname{erf} \left(\frac{x - \mu_1}{\sigma_1\sqrt{2}} \right) \right]^{n-1} e^{-\frac{1}{2} \left(\frac{x - \mu_1}{\sigma_1} \right)^2} \quad (13)$$

and :

$$f_{\xi_2(k=n)}(x) = \frac{n}{2\sigma_2\sqrt{2\pi}} \left[1 - \operatorname{erf} \left(\frac{x - \mu_2}{\sigma_2\sqrt{2}} \right) \right]^{n-1} e^{-\frac{1}{2} \left(\frac{x - \mu_2}{\sigma_2} \right)^2} \quad (14)$$

B. M-HSD algorithm limits

- **High SNR case:** if the signal is received at a good SNR, the performance of the cyclic test will be ideal (P_{fag} close to zero and P_{dg} close to one where P_{fag} and P_{dg} are respectively the observed false alarm and detection probability of the cyclostationary block). So the saved values in each buffer will be from the same population (signal in $buffer_2$ and noise in $buffer_1$). The variables ξ_1 and ξ_2 will never meet and ξ_1 will always be smaller than ξ_2 . This is due to the fact that the signal is well separated from the noise as shown in Figure 10, which represents the variation of the probability density function of ξ_1 and ξ_2 for different number of iterations at 0 dB. Figure 11 represents the expected values of the distribution of ξ_1 under H_0 and ξ_2 under H_1 over the number of iterations (obtained using (14) and (13)). It is clear that ξ_1 and ξ_2 are not going to meet even after a huge number of iterations (10^9 iterations, Cf. Figure 10). Then after the convergence of the M-HSD algorithm, the cyclic block will be very rarely used because it is very rare that the statistic X_i falls between ξ_1 and ξ_2 leading to a radiometer complexity and to perfect decisions.

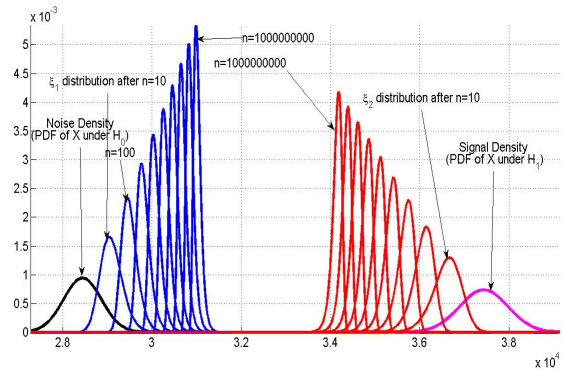


Fig. 10. The variation of the probability density function of ξ_1 (resp. ξ_2) under H_0 (resp. H_1) for different number of iterations at 0 dB, plotted using (13) (resp. (14)).

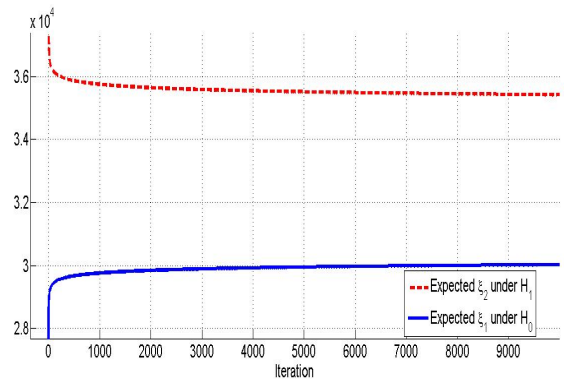


Fig. 11. The expected values of ξ_1 (resp. ξ_2) under H_0 (resp. H_1) as function of the iterations number n at 0 dB, plotted using a numerical calculus using (13) (resp. (14)) and the Matlab tool.

- **Low SNR case:** If the signal is received at a low SNR, the received signal will be very close to the noise level, then ξ_2 will soon be less than ξ_1 after a small number of iterations as we can see in Figure 12. Moreover, with low SNR, the cyclic test can easily misdetect in its decisions (for example the values saved in the buffers may not be from the same population). In this case, it would be better to change ξ_2 instead of changing ξ_1 . This fact induces a strong degradation of the detection performance. Once ξ_1 becomes greater than ξ_2 , the M-HSD algorithm will fix $\xi_1 = \xi_2$ and will stop its evolution. In this case the M-HSD algorithm has reached its detection limit.

VI. THE ENHANCED HSD ALGORITHM (EHSD)

An Enhanced architecture of this last one can be studied as well to improve the detection at lower SNR. It consists in directly estimating the noise level \hat{N}_0 . We will keep the same algorithm of the M-HSD architecture but with just making few modifications: N_1 will be chosen to be big enough to make a good estimation of the noise level N_0 . Moreover, we will keep ξ_2 in the architecture to reduce the detection complexity as much as possible. Directly when $buffer_1$ is full, we will calculate its mean $\hat{\mu}_1$. Then, the EHSD algorithm will use the

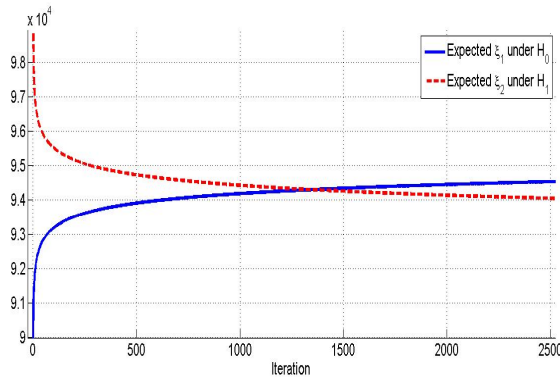


Fig. 12. The expected values of ξ_1 (resp. ξ_2) under H_0 (resp. H_1) as function of the iterations number n at -10 dB, plotted using a numerical calculus using (39) (resp. (40)) and the Matlab tool. We can observe that ξ_2 will soon be less than ξ_1 after a small number of iterations at low SNR .

following equation to estimate N_0 :

$$\hat{N}_0 = \frac{\hat{\mu}_1}{BT}$$

Using this estimation of \hat{N}_0 , we can estimate $\hat{\xi}_0$ that guarantees the $P_{fa,des}$ from the equation bellow:

$$\hat{\xi}_0 = G(P_{fa,des})\hat{N}_0$$

EHSD is a little more complex than M-HSD, because we will need to repeat the cyclostationary test at least N_1 times to be able to estimate $\hat{\xi}_0$, (the size of $buffer_1$ in the EHSD algorithm is usually bigger than the size of $buffer_1$ in the M-HSD algorithm). Figure 13 shows the algorithm of the EHSD method.

A. EHSD Performance

Let D_0 (resp. D_1) designate the event that the cyclic detector has chosen H_0 (resp. H_1). If we assume that for a given SNR the cyclic detector can make false alarms under H_0 and good detections under H_1 independently of the value of the calculated variable X , then we can write:

$$E(X|H_1, D_0) = \mu_2 \quad (15)$$

and

$$E(X|H_0, D_0) = \mu_1 \quad (16)$$

where $E(\cdot)$ denotes the expectation operator.

Recall the partition probability theorem stated below:

$$E(X|D_0) = P(H_1|D_0)E(X|H_1, D_0) + P(H_0|D_0)E(X|H_0, D_0)$$

Using the assumptions of (15) and (16), we can write:

$$E(X|D_0) = P(H_1|D_0)\mu_2 + P(H_0|D_0)\mu_1 \quad (17)$$

by applying Bayes equality we can write:

$$P(H_1|D_0) = \frac{P(D_0|H_1)P(H_1)}{P(D_0)} \quad (18)$$

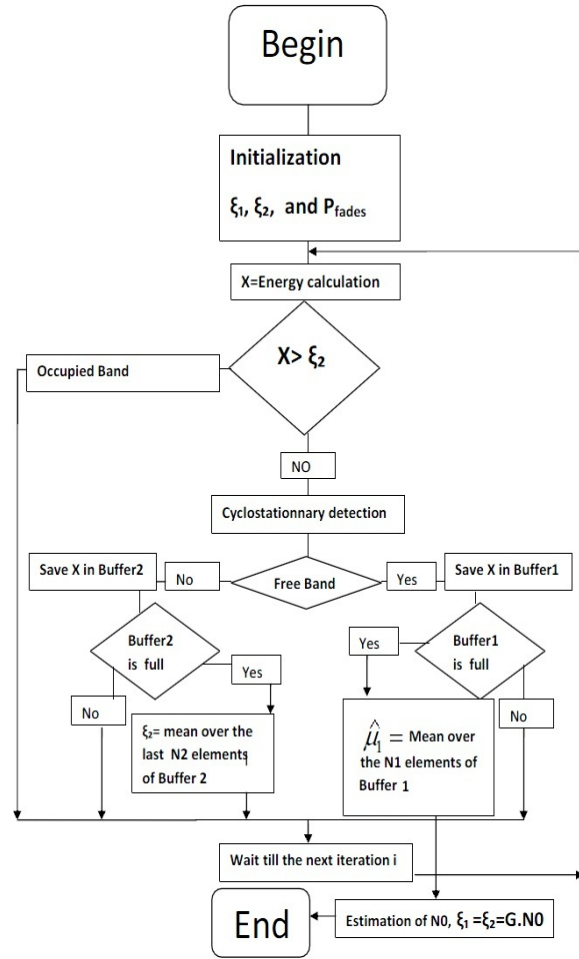


Fig. 13. Algorithm of the EHSD architecture. Only few modifications over the M-HSD algorithm are done.

$$P(H_0|D_0) = \frac{P(D_0|H_0)P(H_0)}{P(D_0)} \quad (19)$$

We can express the probability that the cyclic detector chooses H_0 in terms of $P(H_1)$, $P(H_0)$, $P_{fa,g}$, and P_{dg} :

$$P(D_0) = (1 - P_{fa,g})P(H_0) + (1 - P_{dg})P(H_1) \quad (20)$$

now considering the following definition:

$$\gamma = \frac{P(H_0)}{P(H_1)}$$

where γ represents the characteristic of the environment (free or occupied). Using (18), (19) and (20), equation (17) becomes:

$$E(X|D_0) = (1 - \delta)\mu_2 + \delta\mu_1 \quad (21)$$

where

$$\delta = \frac{1 - P_{fa,g}}{1 - P_{fa,g} + \frac{1 - P_{dg}}{\gamma}}$$

Or for all δ we have:

$$(1 - \delta)\mu_2 + \delta\mu_1 \geq \mu_1$$

Therefore we conclude that:

$$E(X|D_0) \geq \mu_1$$

This means that we always have an over estimation of the noise level N_0 ($\hat{\xi}_0 \geq \xi_0$), which implies that the false alarm constraint will always be respected in the EHSD method (the observed false alarm is then less or equal to the desired false alarm). Using (21) we can find a theoretical approximation for the expression of the relative error over the estimated threshold $\hat{\xi}_0$ defined by $Error_{rel} = \frac{\hat{\xi}_0 - \xi_0}{\xi_0}$, as function of the SNR.

For large N_1 , we can write:

$$\hat{\mu}_1 \approx E(X|D_0)$$

then:

$$\hat{N}_0 \approx \frac{E(X|D_0)}{TW}$$

Using the result given by (21) we can write:

$$\hat{N}_0 \approx \frac{(1 - \delta)\mu_2 + \delta\mu_1}{TW}$$

so $Error_{rel}$ can be approximated by:

$$Error_{rel} \approx \frac{\frac{G}{TW}((1 - \delta)\mu_2 + \delta\mu_1) - \frac{G}{TW}\mu_1}{\frac{G}{TW}\mu_1}$$

after simplifying it, we will obtain:

$$Error_{rel} \approx \frac{SNR}{\gamma \frac{1 - P_{fa}}{1 - P_{dg}} + 1} \quad (22)$$

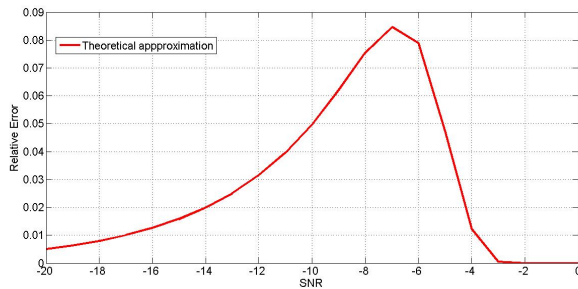


Fig. 14. The theoretical approximation of the relative error over the threshold ξ_0 , simulated using the approximation (22).

Observing the curve in Figure 14, we can check that for high SNRs (when the cyclic test is perfect), the term $1 - P_{dg}$ goes to zero as well as global expression of $Error_{rel}$. In that case, an excellent estimation of ξ_0 can be done. For lower SNR, the term $1 - P_{dg}$ is not zero anymore because the cyclostationary test is no more an ideal test inducing an error over the estimation of ξ_0 . This error reaches its maximum before it starts to decrease because the SNR term becomes very small. Physically this error reduction is due to the fact that the signal is too weak and thus close to the noise level.

VII. SIMULATION RESULTS AND DISCUSSION

In the simulations, we used a 4-PSK modulation at 20 KHz where $\alpha = \frac{1}{T_s}$ is the cyclic frequency used in the cyclostationary detector *a priori* known, and T_s refers to the symbol period of the 4-PSK. We set N_1 and N_2 equal to 30 in the simulation of the M-HSD algorithm, while for the EHSD algorithm, we used $N_1 = 100$ and $N_2 = 30$. The time-bandwidth product BT is equal to 4500 and an equiprobabilist environment ($\gamma = 1$) was used, unless otherwise stated while simulating the different architectures.

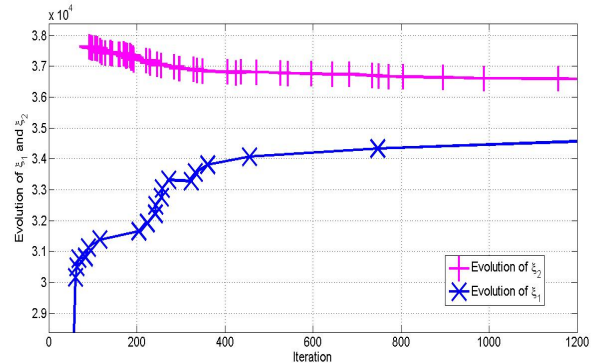


Fig. 15. The variation of ξ_1 and ξ_2 at -5 dB using M-HSD algorithm, with $\gamma = 1$, $N_1 = 30$, and $N_2 = 30$. Each mark on the curves indicates a modification of ξ_1 and ξ_2 . One can notice that the cyclostationary test is less and less used, as the number of iterations increases, inducing a lower complexity.

Figure 15 presents the evolution of ξ_1 and ξ_2 over the iterations of the M-HSD algorithm at -5 dB. We have fixed ξ_G to guarantee a P_{fa} less than 1%. Each mark on the curves in Figure 15 indicates a modification of ξ_1 or ξ_2 . We can observe that there are lots of marks at the beginning, which means that the cyclostationary test is frequently used at this stage, but after a while, the cyclostationary test is much less utilised inducing a lower complexity.

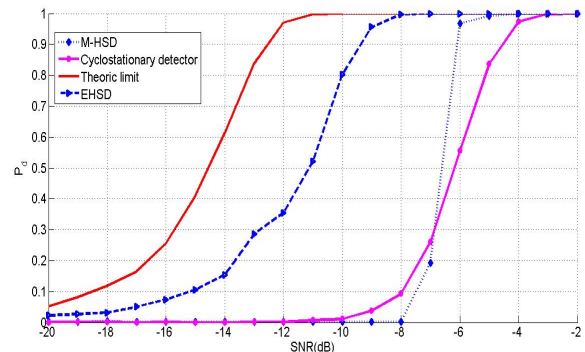


Fig. 16. Simulated detection probability as function of SNR of the M-HSD (using $N_1=N_2=30$), and EHSD (using $N_1=100$, and $N_2=30$) architectures with a $P_{fa,des}$ fixed at 1%, also compared to the cyclic test and to the ideal radiometer under the same conditions.

In order to compare detection performances of the different above mentioned techniques, we simulate the variation of the

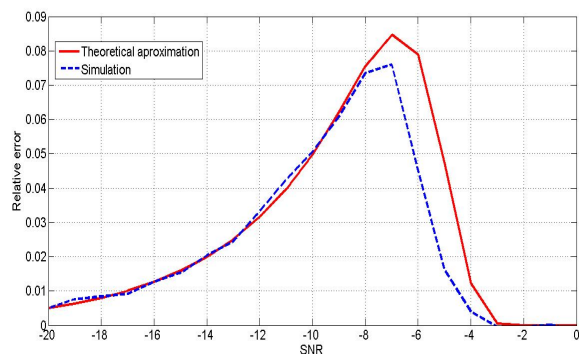


Fig. 17. Simulation result of the relative error of the estimated threshold $\hat{\xi}_0$ as function of the SNR using the EHSD algorithm, compared to the theoretical approximation given in (22).

probability of detection as function of SNR , for the M-HSD and EHSD, using the same $P_{fa,des} = 1\%$. We also compare the obtained results with the curves representing the performance of the cyclic test and the ideal radiometer. The simulated results are shown in Figure 16, where we can observe that the performance of the M-HSD algorithm are near the cyclostationary detector, which means that M-HSD has reached the performance of the cyclic test with a radiometer complexity. Now if we take a look at the EHSD algorithm performance, which also has a radiometer complexity at steady state, we can see that it is able to detect at 100%, with an observed P_{fa} smaller 1% starting at -8 dB, versus -3 dB for the cyclic test, and so achieving a gain of 5 dB in terms of SNR . It should be noted that the EHSD algorithm is a little more complex than M-HSD algorithm at the beginning of the sensing process since it needs a larger $buffer_1$ to achieve a good estimation of N_0 .

Figure 17 validates the approximation given in (22) of the relative error of the threshold $\hat{\xi}_0$ as function of the SNR . This approximation is very close to the simulation results especially at low and high SNR . It can be concluded that when the cyclostationary test starts detecting at 100% (at -3 dB), we can have then a perfect estimation of ξ_0 . An important remark is that for example, at -8 dB, we have a maximum error over the threshold estimation and we can still detect at 99% (Cf. Figure 16). This fact is explained by Figure 18, that shows the PDF of X under both, H_0 and H_1 at -8 dB using (7). We can observe that these densities are still well separated at -8 dB. In consequence this error of estimation does not have a significant impact over the detection performances. At the matter of fact we can observe that $\hat{\xi}_0$ is located on the tail of the PDF of X under H_1 .

A. The Influence of the Environment γ over the Performance of the M-HSD and EHSD Algorithms

As we have already seen, the state of the channel (free or occupied) can be characterized by the variable γ as the ratio between $P(H_0)$ and $P(H_1)$. If we look closely at Figure 12, we note that the point of intersection of the two curves

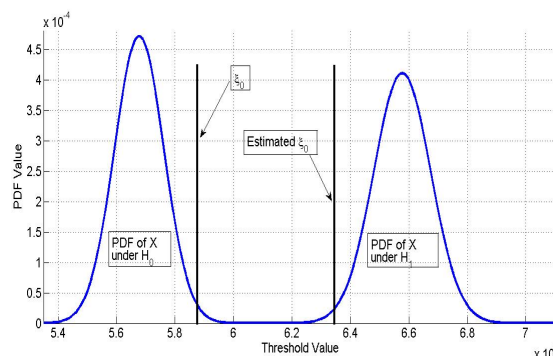


Fig. 18. The distribution of the statistic X under the two hypothesis H_0 and H_1 obtained using (7) of Urkowitz at -8 dB. We have found that in this situation $\hat{\xi}_0$ is located on the tail of the PDF of X under H_1 , that is why we can still obtain good detection performance although the estimation error over ξ_0 is maximal.

that presents the expectation of ξ_1 and ξ_2 , under respectively H_0 and H_1 , does not depend solely on the SNR of the received signal but also on how the sequence of the events *free channel* or *occupied channel* is occurring while using the M-HSD algorithm. Also if we look at (22), which gives the relative error in estimating the optimal threshold when using the EHSD algorithm, we can check that it depends also on the environment characteristic γ . This is the reason why it is interesting to observe the influence of the environment over the performance of our different proposed architectures.

We have used two extreme simulation environments to observe the variation of the performance of the M-HSD detector. The first is $\gamma = 99$ ($P(H_0) = 99\%$) and the second is $\gamma = 0.01$. We observe in Figure 19 that the performance effectively varies depending on the environment γ . For $\gamma = 99$, which signifies that 99% of the time the band is free, ξ_1 keeps increasing, causing a reduction of the detection performance. This environment ($\gamma \gg 1$) is not that one favorable for the M-HSD algorithm because it will have its detection performance close to the cyclostationary detector (at -4 dB M-HSD detects up to 100% versus -3 dB for the cyclic detector), so the major advantage in this case is the lower complexity of the M-HSD algorithm.

However, when $\gamma = 0.01$ ($P(H_1) = 99\%$) ξ_2 keeps decreasing, which allows better detection results. In this case a gain of 2 dB is observed compared to the cyclic detector. Moreover M-HSD is still less complex, and detects significantly better than the cyclostationary detector. Then, we conclude that the M-HSD algorithm ensures a gain between one and two dB over the detection performance of the cyclic detector with a decreasing complexity.

Now we simulate the EHSD architecture in both environments, $\gamma = 99$ and $\gamma = 0.01$. For $\gamma = 99$, the observed performance in Figure 20 is close to the ideal radiometer performance. This result is explained in (22), which shows that the relative error is inversely proportional to γ . So for $\gamma = 99$ this error is almost zero for all the SNR . Therefore the

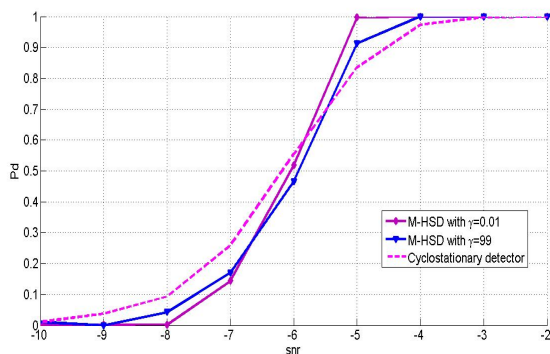


Fig. 19. Simulated detection probability under different SNRs, of the M-HSD (using $N_1=N_2=30$), with $P_{fa,des}$ fixed at 1% using $\gamma = 99$ and $\gamma = 0.01$, also compared to Giannakis test under the same conditions.

estimated threshold $\hat{\xi}_0$ is very close to the optimal threshold ξ_0 , which explains the obtained result. As for $\gamma = 0.01$, the same formula (22) shows that for low SNR the relative error over the estimation of the optimal threshold is high because γ is less than 1. But for high SNR , we have P_{dg} close to one, which makes the relative error decreases to zero. Then we can observe that the performance of the EHSD is always better than that of the M-HSD algorithm. In fact there is always a minimum gain of 2 dB over the cyclic detector, and if the environment is favorable ($\gamma \gg 1$) to the EHSD algorithm, we may even reach the performance of the ideal radiometer.

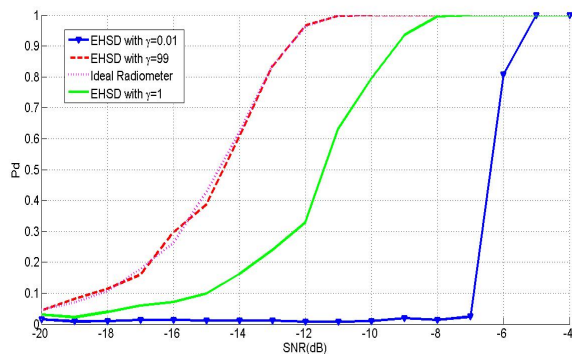


Fig. 20. Simulated detection probability under different SNRs, of the EHSD (using $N_1=100$, and $N_2=30$), with $P_{fa,des}$ fixed at 1% using $\gamma = 99$, $\gamma = 1$ and $\gamma = 0.01$, also compared to the ideal radiometer under the same conditions.

Another way of comparing performance is to plot the ROC curves already defined in part II. For $\gamma = 1$, we simulate for different SNR s the ROC curve of both M-HSD and EHSD. For a relatively good SNR (-5 dB), we can check in Figure 21 that both architectures present the same performance. But for lower SNR (-10 dB), we can observe in Figure 22 the superiority of the EHSD over the M-HSD algorithm in terms of detection. Although both EHSD and M-HSD converge to a radiometer complexity at steady state, EHSD has always better performance than M-HSD. Therefore it is better to use EHSD instead of M-HSD.

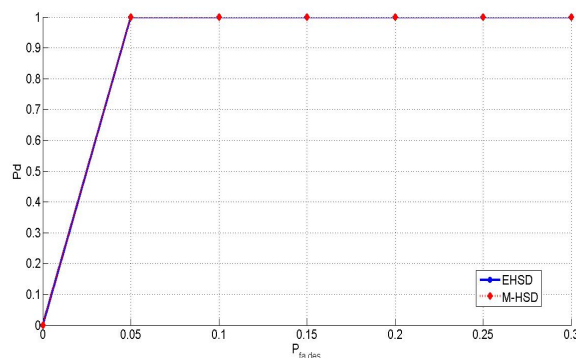


Fig. 21. ROC curves of the M-HSD and the EHSD at -5 dB, for $\gamma = 1$. We observe that in these conditions M-HSD and EHSD present the same performance.

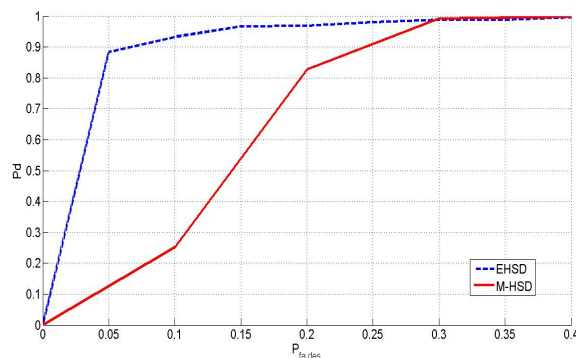


Fig. 22. ROC curves of the M-HSD and the EHSD at -10 dB, for $\gamma = 1$. We observe that in these conditions EHSD presents better detection performance compared to M-HSD.

VIII. CONCLUSION

Spectrum sensing is subject to time constraints. For this reason, we have proposed adaptive architectures, which combine two systems. The first system is a low complexity detector, but it is very sensitive to a bad estimation of the noise level N_0 . As for the second, it is a more complex system based on cyclostationary detection, but it is insensitive to a poor estimation of N_0 . These new adaptive architectures allow the sensing at lower SNR and with a decreasing algorithmic complexity. In a Gaussian noise environment the obtained results are promising as it was shown by the performed simulations. Future work will include the study of different channel types with a variable N_0 . A study of the convergence time and power consumption of the proposed architectures are under investigation.

ACKNOWLEDGMENT

The authors would like to thank Wassim Jouini for his comments and insightful discussions regarding this work.

REFERENCES

- [1] Z. Khalaf, A. Nafkha, J. Palicot, and M. Ghazzi, *Hybrid Spectrum Sensing Architecture for Cognitive Radio Equipment*, AICT'10, May 2010, Barcelona, Spain.

- [2] J. Mitola, *Cognitive Radio An Integrated Agent Architecture for Software Defined Radio*, PhD thesis, Royal Institute of Technology (KTH), May 2000.
- [3] Spectrum Efficiency Working Group. Report of the Spectrum Efficiency Working Group. Technical report, FCC, November 2002.
- [4] Y. Zeng, Y. Liang, A. T. Hoang, and R. Zhang, *A Review on Spectrum Sensing for Cognitive Radio: Challenges and Solutions*, EURASIP Journal on Advances in Signal Processing Volume 2010, Article ID 381465, October 2009.
- [5] S. M. Kay, *Fundamentals of Statistical Signal Processing: Detection Theory*, vol. 2, Prentice Hall, Upper Saddle River, NJ, USA, 1998.
- [6] P.M. Fishman, *Radiometric detection of spread-spectrum signals in noise of uncertain power*, *IEEE Transactions on Aerospace and Electronic Systems*, vol. 28, pp. 654-660, July 1992.
- [7] H. Urkowitz, *Energy detection of unknown deterministic signals*, *Proceedings of the IEEE*, vol. 55, no. 4, pp. 523-531, 1967.
- [8] H. S. Chen, W. Gao, and D. G. Daut, *Signature based spectrum sensing algorithms for IEEE 802.22 WRAN*, in *Proceedings of the IEEE International Conference on Communications (ICC 07)*, pp. 6487-6492, Glasgow, Scotland, June 2007.
- [9] M. Ghozzi, *Détection cyclostationnaire des bandes de fréquences libres*. PhD thesis, 2008.
- [10] W.A. Gardner and C.M. Spooner, *Signal interception: Performance advantages of cyclic feature detectors*, *IEEE Transaction on Communications*, vol. 40, January 1992.
- [11] W.A. Gardner and G. Zivanovic, *Degrees of cyclostationary and their application to signal detection and estimation*, *Signal processing*, vol. 22, March 1991.
- [12] W. A. Gardner, *Exploitation of spectral redundancy in cyclostationary signals*, *IEEE Signal Processing Magazine*, vol. 8, no. 2, pp. 14-36, 1991.
- [13] A.V. Dandawate and G.B. Giannakis, *Statistical tests for presence of cyclostationarity*, *IEEE Transactions on Information Theory*, vol. 42, pp. 2355-2369, September 1994.
- [14] Y. H. Zeng and Y.-C. Liang, *Eigenvalue-based spectrum sensing algorithms for cognitive radio*, *IEEE Transactions on Communications*, vol. 57, no. 6, pp. 1784-1793, 2009.
- [15] F. Penna, R. Garello, and M. A. Spirito, *Cooperative spectrum sensing based on the limiting eigenvalue ratio distribution in wishartmatrices*, *IEEE Communications Letters*, vol. 13, no. 7, pp. 507-509, 2009.
- [16] L. S. Cardoso, M. Debbah, P. Bianchi, J. Najim, *Cooperative Spectrum Sensing Using Random Matrix Theory*, invited paper, Proc. ISWPC 2008, May 2008, Santorini, Greece.
- [17] Z. Tian and G. B. Giannakis, *A wavelet approach to wideband spectrum sensing for cognitive radios*, in *Proceedings of the 1st International Conference on Cognitive Radio Oriented Wireless Networks and Communications (CROWNCOM 07)*, Mykonos, Greece, June 2007.
- [18] Y. H. Zeng and Y.-C. Liang, *Spectrum-sensing algorithms for cognitive radio based on statistical covariances* *IEEE Transactions on Vehicular Technology*, vol. 58, no. 4, pp. 1804-1815, 2009.
- [19] Y. H. Zeng, Y.-C. Liang, and R. Zhang, *Blindly combined energy detection for spectrum sensing in cognitive radio*, *IEEE Signal Processing Letters*, vol. 15, pp. 649-652, 2008.
- [20] A. Sahai, S. M. Mishra, R. Tandra, and K. A. Woyach, *Cognitive radios for spectrum sharing*, *IEEE Signal Processing Magazine*, vol. 26, no. 1, pp. 140-145, 2009.
- [21] H.L. Van Trees, *Detection, estimation, and modulation theory, Part III*. Wiley, 1971.
- [22] D. Middleton, *Canonically optimum threshold detection*, *IEEE Transactions on information Theory*, vol. 12, pp. 230-243, April 1966.
- [23] B. Zayen, A. Hayar, K. Kansanen, *Blind Spectrum Sensing for Cognitive Radio Based on Signal Space Dimension Estimation*, ICC'09, IEEE International Conference on Communications, June 14-18, 2009, Dresden, Germany.
- [24] W.A. Gardner, *Introduction to random processes with applications to signals and systems*. New York : McGraw-Hill, 1989.
- [25] L. Izzo, L. Paura and M. Tanda, *Signal interception in non-gaussian noise*, *IEEE Transaction on Communications*, vol. 40, pp. 1030-1037, June 1992.
- [26] P. Rostaing, *Détection de signaux modulés en exploitant leurs propriétés cyclostationnaires : Application aux signaux sonar*. PhD thesis, Université de Nice - Sophia Antipolis, 1997.
- [27] H.L. Hurd and N.L. Gerr, *Graphical methods for determining the presence of periodic correlation* *Journal of Time Series Analysis*, vol. 12, no. 4, pp. 337-350, 1991.
- [28] M. Öner and F. Jondral, *Air interface recognition for a software radio system exploiting cyclostationarity*, in *Proc. IEEE PIMRC'04*, Barcelona, Spain, vol. 3, pp. 1947-1951, September 2004.
- [29] M. Öner and F. Jondral, *Extracting the channel allocation information in a spectrum pooling system exploiting cyclostationarity*, in *Proc. IEEE PIMRC'04*, vol. 1, pp. 551-555, September 2004.
- [30] A. Papoulis and S.U.Pillai, *Probability, Random Variables and Stochastic Processes*, Mc Graw Hill, 2002.